PROTEINS
STRUCTURE ■ FUNCTION ■ BIOINFORMATICS

New insight into the architecture of oxy-anion pocket in unliganded conformation of GAT domains: A MD-simulation study

Hridoy R. Bairagya* and Manju Bansal

Molecular Biophysics Unit, Indian Institute of Science, Bangalore, Karnataka, 560012, India

ABSTRACT

Human Guanine Monophosphate Synthetase (hGMPS) converts XMP to GMP, and acts as a bifunctional enzyme with N-terminal "glutaminase" (GAT) and C-terminal "synthetase" domain. The enzyme is identified as a potential target for anti-cancer and immunosuppressive therapies. GAT domain of enzyme plays central role in metabolism, and contains conserved catalytic residues Cys104, His190, and Glu192. MD simulation studies on GAT domain suggest that position of oxyanion in unliganded conformation is occupied by one conserved water molecule (W1), which also stabilizes that pocket. This position is occupied by a negatively charged atom of the substrate or ligand in ligand bound crystal structures. In fact, MD simulation study of Ser75 to Val indicates that W1 conserved water molecule is stabilized by Ser75, while Thr152, and His190 also act as anchor residues to maintain appropriate architecture of oxyanion pocket through water mediated H-bond interactions. Possibly, four conserved water molecules stabilize oxyanion hole in unliganded state, but they vacate these positions when the enzyme (hGMPS)-substrate complex is formed. Thus this study not only reveals functionally important role of conserved water molecules in GAT domain, but also highlights essential role of other non-catalytic residues such as Ser75 and Thr152 in this enzymatic domain. The results from this computational study could be of interest to experimental community and provide a testable hypothesis for experimental validation. Conserved sites of water molecules near and at oxyanion hole highlight structural importance of water molecules and suggest a rethink of the conventional definition of chemical geometry of inhibitor binding site.

Proteins 2016; 84:360–373.

Key words: oxyanion hole; conserved water molecules; MD-simulation; hGMPS enzyme.

INTRODUCTION

In de novo biosynthesis of purine nucleotides, Inosine Monophosphate (IMP) is the branch point metabolite that directs the synthesis of either guanine or adenine nucleotides.[1] In guanine nucleotide pathway, Inosine Monophosphate Dehydrogenase (hIMPDH, EC 1.1.1.2051) catalyzes the oxidation of IMP to produce XMP (xanthine monophosphate), while Guanine monophosphate synthetase (hGMPS, EC 6.3.5.2) converts that XMP to GMP (guanosine monophosphate).[2] Subsequently, both these enzymes are involved in cellular metabolism pathways that exhibit elevated levels of activity in rapidly proliferating cells, such as neoplastic and regenerating tissues.[3,4] Inhibition of hGMPS has been shown to result in control of cell growth[5] and the enzyme has been identified as a potential and attractive drug target for anticancer, immunosuppressive and antiviral chemo-therapies.[6,7] Several glutamine analogues like acivicin [(αS,5S)-α-amino-3- chloro-4,5-dihydro-5-isoxazoleacetic acid], DON (6-diazo-5-oxo-L-norleucine) and azaserine (O-diazoacetyl-L-serine) were earlier investigated as cancer chemotherapeutic agents, but these compounds were shown to cause cellular cytotoxicity in human somatic cell.[8,9]hGMP synthetase exists as a homodimer in the crystal and acts as a glutamine dependent amidotransferase. Surprisingly, hGMPS also

Additional Supporting Information may be found in the online version of this article.

Grant sponsor: Science and Engineering Research Board (Department of Science and Technology, Govt. of India); Grant number: SB/FT/CS-051/2012.

Hridoy R. Bairagya current address is Department of Chemistry, Lensfield Road, University of Cambridge, Cambridge, CB2 1EW

*Correspondence to: Dr. Hridoy Ranjan Bairagya; Molecular Biophysics Unit, Indian Institute of Science, Bangalore, Karnataka 560012, India.

E-mail: hrb45@cam.ac.uk or hbairagya@gmail.com

Received 16 September 2015; Revised 6 December 2015; Accepted 19 December 2015

Published online 28 January 2016 in Wiley Online Library (wileyonlinelibrary.com). DOI: 10.1002/prot.24983

functions as a bifunctional enzyme with two distinct functional domains: N-terminal "glutaminase" (GAT) or "amidotransferase" domain, which is responsible for abstraction of amide nitrogen from substrate or glutamine to produce ammonia, which is then transferred to C-terminal "synthetase" domain (~23 Å from GAT domain) for aminating XMP to yield GMP.[7] This transportation of ammonia within the enzyme (ammonia channelling) is an interesting feature of amidotransferases.[10] To synthesize GMP, the enzyme can utilize either ammonia or glutamine as the source of nitrogen.[11] Crystallographic structures (from both prokaryotic and eukaryotic sources) show that the GAT domain of hGMPS is composed of a central β-sheet surrounded by α-helices, which contains the conserved catalytic residues Cys104, His190 and Glu192.[7] Biochemical and physical studies have demonstrated that Cys104 is an active site residue, essential for GAT function, whereas His190 serves as a general base involved in the nucleophilic attack on Cys104.[12] The nucleophilic sulfhydryl sidechain of the cysteine residue initiates amide transfer by forming a thioester in the presence of substrate glutamine. The enzyme hGMPS reversibly adenylates XMP to form a covalent O^{2-} adenyl-XMP intermediate, which activates the C^2 carbon of XMP attack via amide nitrogen of glutamine. If the nitrogen source is absent, then that covalent intermediate is slowly hydrolyzed to form XMP and AMP.

A tight α/β connection (similar to α/β hydrolase) is described as a nucleophile elbow, that is observed in GMPS enzyme and consists of Cys104 (perched at tip of elbow), Gly102 (last residue of a β-strand) and Gly106 (first residue of an α-helix). Again, the oxyanion hole of hGMPS (Class-I amidotransferase) is formed by backbone nitrogen atoms of Tyr105 and Gly77 residues, which also stabilize transient negative charge on the glutamine amide oxygen of substrate to form a tetrahedral intermediate. Thus, the nucleophile, oxyanion hole and His190 (proton donor) of hGMPS form a binding site for the amide plane of the substrate glutamine. Interestingly, location of binding site of glutamine substrate determines whether nucleophile attack by Cys104 is toward *Re* or *Si*-face of amide plane. *Re*-face binding mode of substrate appears to be blocked by the enzyme core, whereas *Si* face may be an alternative way of attack by Cys104.[13] Despite the apparent catalytic readiness of Cys104, GAT domain has very poor glutaminase affinity in the absence of substrate XMP and ATP (in the synthetase domain). Some conformational changes have been reported to occur after binding of the ligands or acceptor at synthetase domain.[14] These may force the GAT domain (specially the catalytic triad) to switch from a non functional to a functional conformation and allow the substrate (Gln) to bind regeospecially in respective GAT domain (Supporting Information Fig. S1). Recently, the mechanism of activation of GATs in GMPS enzyme has been investigated by different groups and they suggest that subunit interfaces may play an important role in GATase activation.[15–18] However, site directed mutagenesis study of carbamoyl phosphate synthetase in *Escherichia coli* indicates some catalytic role of Asn311 and Ser47 in GAT domain.[19] Crystal structures of hGMPS (PDB Id: 2VPI and 2VXO), *Ec*GMPS (PDB Id. 1GPM), *Tt*GMPS (PDB Id. 2YWB), and *Tt*CTPS (PDB Id.1VCO) also provide some clues toward the orientation of Cys104 and geometry of oxyanion pocket with a water molecule inside the primary catalytic zone of GAT domain.[7,13,20] In fact Gln containing GAT structure with bound water molecule at oxyanion pocket is not available to date for hGMPS enzyme, so 1VCO (PDB Id.) in *Tt*CTPS is used in this computational study, because it is the only available crystal structure which contains Gln as substrate in the GAT domain and shows H-bonding interaction with the oxyanion pocket.

Conserved water molecules play a vital role in protein structure, enzyme catalysis, protein architecture, conformational stability, protein plasticity, ligand binding and its selectivity for specific interaction.[21–23] Consequently, X-ray structures of hGMPS provide insufficient insight about the structural and functional importance of conserved water molecules in the vicinity of the oxyanion pocket, when the substrate or ligand is absent in the GAT domain. In this context, it is really difficult to understand the chemical mechanism of oxyanion pocket, its stabilization, dynamic behavior, role of water molecules inside the pocket and participation of non catalytic resides. Hence the approach of MD-simulation, with explicit solvent, of the GAT domain is the only option that may provide this important information about the oxyanion pocket. In spite of this, no MD simulation study (on dynamics of water molecules) has been reported on unliganded conformation of GAT domain in hGMPS enzyme. In addition, the biochemical function of Ser75 and Thr152 (associated residues of oxyanion hole which are located ~5 to 6 Å away from the pocket) has not been investigated experimentally. However, a mutation study of carbamoyl phosphate synthetase (*Escherichia coli)* has indicated the importance and catalytic function of Asn311 and Ser47, which are structural equivalents of Ser75 and Thr152 in hGMPS enzyme. So, these residues of GAT domain may have some catalytic role, that is still unknown, in the forum of hGMPS enzymes. In the current situation, it remains a formidable challenge for us to obtain a better model structure in the unliganded state. To accomplish this, we have performed MD simulations for time scales raging from 25 to 50 ns to investigate the involvement of non catalytic residues (Thr152, Ser75) and their water mediated interaction at the oxyanion hole. The mutagenesis and crystallographic studies of catalytic residues in bleomycin hydrolase (papain family) suggest that a tightly bound structurally conserved water molecule stabilizes the loop

near the active site and displacement of that water molecule by mutation of Asn with Val/Ala destabilizes that loop.[24] Consequently, this information inspired us to confirm the structural/functional role of water molecules at oxyanion position by an *in silico* mutation study of Ser75 to Val. The present study is focused around the oxyanion hole (unliganded structure), which is located at the heart of the catalytic domain, hence we chose only the corresponding GAT domain for MD simulation, rather than considering the entire enzyme structure. It is also a mystery as to how some non catalytic residues (Ser75 and Thr152) are associated in recognition of the oxyanion pocket. To the best of our knowledge this is the first study that incorporates the results of MD analysis, focused on the oxyanion pocket and its conformational stability by conserved water molecules, involvement of noncatalytic residues (Ser75 and Thr152) and their water mediated mutual coupling with oxyanion pocket. Hence, our study may guide the development of more specific drugs or modified inhibitors on the basis of different MD conformations and the results may be combined with chemical screening methods to improve and accelerate the discovery of anticancer drugs for hGMPS enzyme.

MATERIALS AND METHODS

Starting structure

Atomic coordinates of five crystal structures of different (GMP and CTP) types of synthetase enzyme were obtained from Protein Data Bank.[25–27] The X-ray structure of 1VCO in TtCTPS, 2VPI and 2VXO in *h*GMPS, 1GPM in *Ec*GMPS and 2YWB in *Tt*GMPS were included in the present study, however those crystal structures have been solved in different space groups and with different resolutions (Supporting Information Table S1). The A molecule of 2VXO and 1VCO, B molecule of 2VPI and 2YWB, and D molecule of 1GMP were separated (including crystal water molecules and inhibitors/ligands) from their respective X-ray structures using Swiss PDB viewer program[28,29] for further analysis. Hence, crystal structure of 2VPI was taken as template or reference because its structural quality in B-chain and resolution (2.40 Å) are more suitable than 2VXO. In addition the isolated GAT structure of 2VPI is similar to the GAT structure of the entire enzyme (2VXO), with a backbone r.m.s.d. of 0.50Å (Supporting Information Fig. S15). Consequently, remaining X-ray structures (resolution range from 2.10 to 2.50 Å) of GMPS/CTPS were taken for validation of and comparative analysis with the MD results of 2VPI structure.

Identification of residues of oxyanion pocket in different X-ray structures

The nucleophile (Cys), catalytic base (His) and other residues constituting elements of the oxyanion hole and its surrounding interactions in five X-ray structures were analyzed using Swiss PDB Viewer program. The side-chain dihederal angle (Chi1) of catalytic Cys residues of five X-ray structures were calculated using STAN program.[30]

Preparation of simulation system

Initial atomic coordinates of the protein (excluding crystal water molecules) were taken from crystal structure of hGMPS (PDB Id: 2VPI) for molecular dynamics simulation. Missing hydrogen atoms were added to the structure using the AutoPSF module of VMD (Visual Molecular Dynamics v.1.9.2.) program.[31] This structure was then solvated in a cubic box of 15,622 TIP3P water molecules extending at least 10 Å from the protein surface. Sodium and chloride ions were used to neutralize the overall charge of the system; the resulting system consisted of 49,867 atoms for starting simulation.

MD simulations

Molecular dynamics of solvated structure was performed using NAMD (Nanoscale Molecular Dynamics v.2.9) program[32,33] with CHARMM-27 force field.[34,35] Initial energy minimization was performed for 1000 steps by fixing the backbone atoms, followed by a second minimization of 1000 steps restraining only the CA atoms of the protein. The water molecules and ions were then equilibrated for 2 ns while constraining the protein. A final minimization of 2000 steps was carried out for all atoms of the system to ensure the removal of any residual steric clashes. A stepwise heating was carried out from 0 to 310 K >3000 steps. Finally, all atom molecular dynamics simulation was performed in the NPT ensemble (constant number of atoms, pressure, and temperature) for a time period of 50 ns. To mimic physiological conditions, the temperature was kept at 310K using Langevin dynamics[36] with a damping coefficient of $5ps^{-1}$. The pressure was maintained at 1 atm using the Langevin piston Nose–Hoover method,[37,38] with a piston period of 100fs and a decay time of 50fs. During simulation, Nose-Hoover Langevin piston barostat and Langevin thermostat were used to control constant pressure and temperature of the system. Periodic boundary conditions and a cutoff distance of 12 Å, switch distance of 10 Å, pairlist distance of 14 Å for van der Waals interactions was applied. The Particle–Mesh Ewald method was used to compute the long-range electrostatic interactions by specifying proper PME grid size. The SHAKE algorithm[39] was used to constrain all bond lengths involving hydrogen atoms which permits a 2 fs time step and the value of step per cycle (timesteps per cycle) was assigned as 10.Simulation was found to converge within 15 ns, and further 35 ns simulation was carried out for production run (Supporting Information Fig. S2). The atomic

coordinates of MD structures (25,000 frames) were recorded at every 2 ps for further analysis.

Root mean-square deviations and atomic fluctuations

Average root mean square deviation (RMSD) of MD structures (25,000 no. of frames) was calculated (X-ray structure was taken as reference molecule) by RMSD trajectory tool in VMD. Root mean square fluctuation (RMSF) of CA atoms during simulation was also calculated to characterize the structural flexibility of GAT domain. For convenient comparison with MD results, the experimental B-factors of crystal structure were converted to RMSF value by using Debye-Waller formula: $(\mathrm{RMSF} = 3B/8\pi^2)^{1/2}$.[40]

Identification of conserved water molecules and their calculation of SASA values

Seven conserved water molecules (W1, WH, W2A, WTA, W2B, WS, WTB) were identified from simulated structures of GAT domain using 3DSS program[41]; in addition the conserved positions of these water molecules were also verified by SPDBV program. During simulation, oxyanion pocket of protein adopts two conformations (1A and 1B). Isolated moieties that contained Ser75, Gly77, Cys104, Tyr105, Thr152, His190, W1, WH, W2A, and WTA were taken for Conformation 1A, whereas Ser75, Gly77, Cys104, Tyr105, Thr152, His190, W1, WH, W2B, WS, WTB were considered as Conformation 1B. Water molecules (oxygen atoms) whose centre to centre distance (indifferent snapshots) was within 1.5 Å[42] in between reference and movable structures,were taken as conserved. Final MD structure (50 ns) of 2VPI was taken as a template/fixed and other prerecorded snapshots (frames from 15 to 50 ns) were assigned as movable and conserved water sites were determined between two respective simulated structures. Moreover, residential frequency of water molecule W1, WH, W2A, and WTA of conformation 1A, and W1, WH, W2B, WS, and WTB of conformation 1B were calculated. In addition, VMD program (SASA script) was used to calculate the average SASA (solvent accessible surface areas) values of aforesaid water molecules using the probe radius of 1.4Å.

Modeling of the mutant protein structure

For understanding the significance of a single amino acid substitution on protein function, knowledge about the 3D structure of protein is very important.[43] MD results have confirmed that Ser75 is involved in stabilizing W1 water molecule. Does Ser75 act as a water supplier to the oxyanion pocket in unliganded form of GAT structure? To address this question, residue Ser75 was mutated to Val in B molecule of 2VPI X-ray structure. The waters were removed, so that the side-chain carbon atom (CG1 or CG2) of Val occupied the position of OG atom of Ser75. Aforesaid mutation was performed using SWISSPDB viewer program, where lowest energy of rotamer was selected for Val75. The mutated residues which were not involved in steric clashes with other residues were included for this study and the overall geometry of the mutant structure was optimized by energy minimization.

Model verification of mutant protein structure and MD simulation

The quality of 3D model structure was assessed by ProSA,[44] Verify 3D,[45] QMEAN,[46] and PROCHECK[47]-program. ProSA calculates energy profiles (z scores) for modeled mutant structure by using molecular mechanics force field. Z-score of Ser75Val of mutated variant is −7.67, which is within the range of scores typically found for proteins of similar groups (Supporting Information Fig. S10). VERIFY-3D program was used to identify unreliable regions in proteins that were improperly modeled, and a 3D model profile was constructed in which each amino acid residue position is characterized by its environmental score. Score of Val75 of mutated amino acid residue was 0.66, compared to the wild type Ser75 with score 0.59. In addition, we have also calculated the 3D-1D averaged score of the mutant structure, 97.4% of the residues has an averaged 3D-1D score >= 0.2 (Supporting Information Fig. S11). However, the QMEAN (a composite scoring function) program was used to derive the global (i.e., for the entire structure) error estimates on the basis of one single model. The normalized QMEAN score of the mutant protein structure is 0.66 (Supporting Information Fig. S12), QMEAN Z score is −1.55 (Supporting Information Fig. S13) and the density plot of QMEAN scores of the reference set is included in Supporting Information Figure S14. All these data derived from different programs, confirm that the good quality of the model mutant structure. This mutant model structure (X-ray structure of Ser75Val) was taken for further MD-simulation study using aforesaid methods. The mutant structure was solvated using solvate module in VMD program and 25 ns simulation was performed by NAMD.

Pocket analysis

The program EPOCK[48] was used to identify and characterize volume of the oxyanion pocket in hGMPS. Sphere method was used to calculate the volume of the pocket by assigning maximum englobing region (MER), where minimum radius of inclusion and exclusion were set to 5 and 10 Å. In addition, the parameters of van der Waals radius, grid spacing and contiguous cutoff were used as 1.4, 0.5, and 4.0 Å. The 500 frames from conformations 1A and 1B were taken after removing all the

Table I
Comparative Analysis of GAT Domains in Different Crystal Structures of GMPS

Type of GMPS	Domain Conformation		Nucleophile	Catalytic Residue	Dihederal angle (°) of catalytic Cys	Residues of Oxyanion hole	Surrounding res.id of Oxyanion hole
	GAT Domain	Synthatase Domain					
*h*GMPS 2VXO 2VPI	unliganded	Absent	Cys104	His190	−169.74 (non functional)	Tyr105 Gly77	Ser75 Thr152
	unliganded	Substrate (XMP)	Cys104	His190	−91.42 (functional)	Tyr105 Gly77	Ser75 Thr152
*Ec*GMPS 1GPM	Ligand (CITRIC ACID)	Substrate (AMP)	Cys86	His78	−57.60 (functional)	Tyr87 Gly59	Ser57 Ser142
*Tt*GMPS 2YWB	unliganded	unliganded	Cys78	His164	−62.92 (non functional)	Tyr79 Gly51	Ser49 Ser125
*Tt*CTPS 1VCO	Substrate (Gln)	unliganded	Cys391	His522	−164.15 (functional)	Leu392 Gly364	Pro362 Arg470

*Amino transferases structurally similar as GAT domain of GMP synthetase.

water molecules to calculate the average volume of the pockets.

RESULTS

Analysis of X-ray structures

The crystal structures of synthatase enzymes were observed in Protein Data Bank either in ligand bound conformation or unliganded form. Since the synthatase domain is absent in the 2VPI structure, the side-chain of active site Cys104 adopts a non functional form (with chi1 value −169.7°) with its SG atom being 3.70 Å away from NE of His190. However, the water molecule W2042 (crystal) in 2VPI structure is observed to bridge the OG of Thr152 and SG of Cys104, thus making the Cys non functional but stabilizing the conformation of side-chain of Cys104 (Table I). Similarly, the non functional form of active site Cys78, with chi1 value of −62.9° was observed in the X-ray structure 2YWB, that also lacks the ligands in both the GAT and synthatase domains. But the thiol group of Cys104 adopts a functional form in the presence of ligands (XMP and ATP) at synthatase domain in 2VXO structure, where the SG atom of Cys104 (chi1 value −91.4°) is also observed to bond with NE of His190 with a separation of 2.9 Å. Superposition of 2VPI and 2VXO structures (Fig. 1) revealed a significant movement of side-chain of Cys104, from its non functional to functional form. Interestingly, the catalytic residues of GAT domain may adopt active conformation in XMP bound state, but conformation of the GAT domain undergoes a transition to the inactive form when XMP moves and vacates the active site on the synthase domain (Fig. 2). Moreover, the thiol group of Cys86 is functional (with chi1 value −57.6°) in 1GPM X-ray structure (*Ec*GMPS), because the GAT and synthatase domain have been occupied by citric acid and substrate (AMP). However, in 1VCO structure the substrate (Gln) was observed at GAT domain with chi1 value of Cys391 being −164.1°. The residues forming the oxyanion hole are Tyr87 and Gly59 in EcGMPS, Tyr79 and Gly51 in TtGMPS; Leu392 and Gly364 in TtCTPS and are also conserved in GMPS enzyme. These residues play an important role in stabilizing the negative charge of oxyanion pocket through water molecule in the ligand free

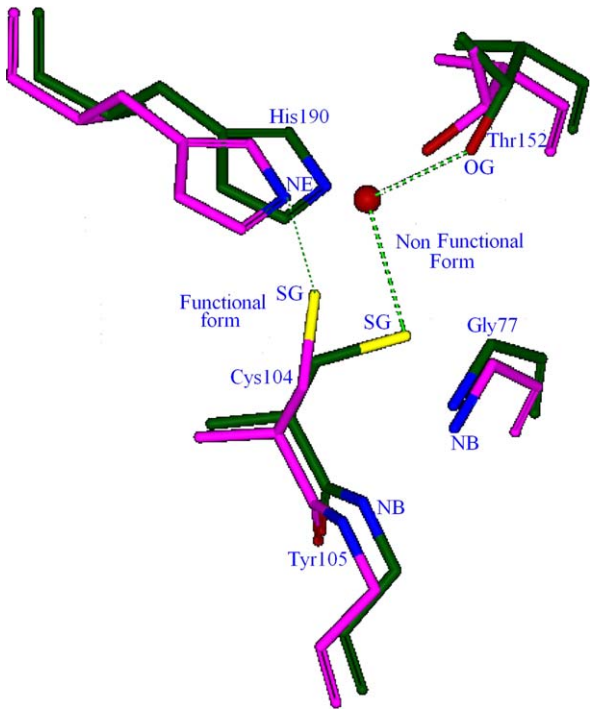

Figure 1
Superimposition of the catalytic residues between two crystal structures (PDB code 2VPI and 2VXO) in hGMPS enzyme to compare the orientation of thiol group (-SH) of Cys104. Cys104 interacts with His190 in 2VXO crystal structure (pink) and stabilizes Thr152 via crystal water molecule W2042 (in B-chain) in 2VPI structure (green). [Color figure can be viewed in the online issue, which is available at wileyonlinelibrary.com.]

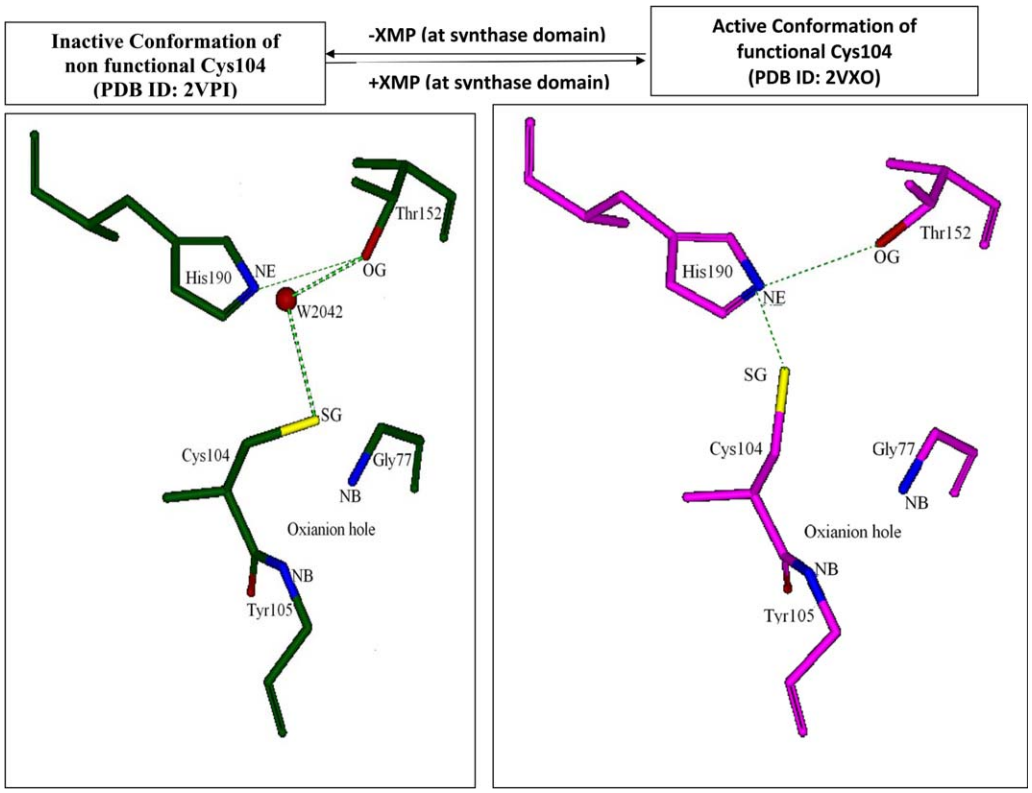

Figure 2

The left (PDB Id. 2VPI, green) and right (PDB Id. 2VXO, pink) panels indicate the non functional and functional conformation of Cys104 residue. It also shows the change in conformation of catalytic residues from inactive to active state, upon binding the XMP at synthase domain. [Color figure can be viewed in the online issue, which is available at wileyonlinelibrary.com.]

conformation and negative charge of the ligands or substrate in ligand bound state. Interestingly, the crystal structure (PDB Id.2YWB) of *Tt*GMPS enzyme contains a water molecule W518 at oxyanion pocket and it interacts with Glu51 and Tyr79 (Supporting Information Fig. S3), but no such bound water molecule at oxyanion position is observed in X-ray structures of other GMPS enzymes. This observation based on X-ray structure of *Tt*GMPS enzyme illustrates and confirms the important role of structural bound water molecule at the position of oxyanion (O^-) atom, inside this pocket at GAT domain (ligand free form). This bound water molecule or hydrophilic center is referred to hereafter as W1.

Analysis of MD trajectories

Role of water molecule inside oxyanion pocket

During MD simulation, we observed that W1 water molecule, that occupies the oxyanion hole of GAT domain, also H-bonds to NB atoms of Tyr105 and Gly77/76. The position of oxygen atom of W1 water molecule is seen to be highly ordered during the entire simulation (15 to 50 ns), and this same position can also be identified in X-ray structure of 2YWB. Hence, the environment around W1 water center (that evolved during simulation) was also compared with unliganded and ligand bound crystal structures of hGMPS enzyme (Table II). In X-ray structure of 2YWB, water molecule W518 (B-value 33.02 $Å^2$) interacts with NB atoms of Gly51 (2.81 Å) and Tyr79 (3.13 Å). The RMSD (backbone) value between 2VPI (MD) and 2YWB (crystal) structure is ~1.28 Å, and their superimposed complex showed that the distance between oxygen atoms of W1 (MD of 2VPI) and W518 (in crystal structure 2YWB) is ~0.77 Å, indicating that these two hydrophilic positions are conserved and are involved in similar type of interactions (Fig. 3). Again, W1 position of 2VPI MD structure is also compared with the ligand bound 1GPM and substrate bound 1VCO X-ray structures. The atom O3 (24.33 Å B-value) of citric acid in 1GPM structure interacts with NB of Gly59 (2.93 Å) and Tyr87 (3.33 Å), similarly OE1 atom of substrate (Gln) in 1VCO structure also interacts with NB of Gly364 (3.17 Å) and Leu392 (3.02 Å). In addition, RMSD (backbone) between 2VPI (MD) and 1GPM and 1VCO structures are ~1.29 and 1.60 Å, respectively, and the corresponding superimposed complexes showed that the distance from oxygen atom of W1 (MD of 2VPI) to O3 of citric acid (in 1GPM structure) and OE1 of Gln (in 1VCO) are

Table II
Comparative Analysis of Oxyanion Hole Between Unliganded MD Structure of hGMPS and Different Crystal Structures of GMPS and CTPS

			Type of GMPS		Type of CTPS
Crystal structure →			TtGMPS (PDB Id: 2YWB) GAT without ligand	EcGMPS (PDB Id:1GPM) GAT with Inhibitor	*TtCTPS (1VCO) Gat with Substrate (Gln)
	RMSD(Å) 2YWBvs 2VPI (Backbone)		1.28	1.29	1.60
Residues of Oxyanion hole	O-	Oxyanion	W518 (Water) **B-value** ($33.02Å^2$)	O3 (Citric acid) **B-value** ($24.33 Å^2$)	OE1 (Gln) **B-value** ($35.94 Å^2$)
	Gly (NB) Tyr/Leu (NB) MD structure of 2VPI (O^{W1}) →	Distance (Å)	$^{W518}O—NB^{Gly51}$ 2.81 $^{W518}O—NB^{Tyr79}$ 3.13 Distance $^{W518}O—O^{W1}$ 0.77Å **(Figure 3)**	$^{CIT}O3—NB^{Gly59}$ 2.93 $^{CIT}O3—NB^{Tyr87}$ 3.33 Distance $^{CIT}O3—O^{W1}$ 0.66Å **(Figure 4)**	$^{Gln}OE1—NB^{Gly364}$ 3.17 $^{Gln}OE1—NB^{Leu392}$ 3.02 Distance $^{Gln}OE1—O^{W1}$ 0.47Å **(Figure 5)**

0.66Å and 0.47 Å (Figs. 4 and 5). These observations clearly reveal that oxygen atom of W1 (MD) in 2VPI, O3 (of citric acid) in 1GPM and OE1 (Gln) in 1VCO are structurally/positionally equivalent. In addition to their geometrical position their pattern of interactions is also conserved in all the corresponding structures.

Analysis of MD conformations

During the entire simulation, the environment (residues) surrounding the oxyanion pocket adopts two conformations (1A and 1B) to stabilize or maintain the topology of this pocket by conserved water mediated H-

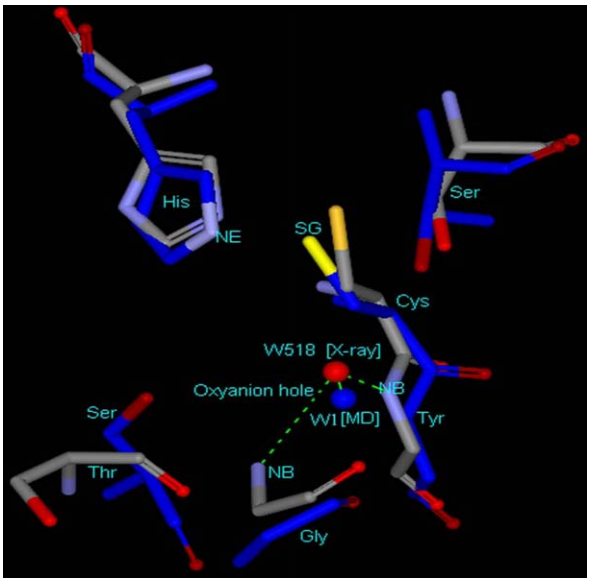

Figure 3
Superimposed (backbone atoms) image of PyGMPS (X-ray, PDB Id: 2YWB) and hGMPS (MD, PDB Id: 2VPI) molecules are shown in CPK and blue colour. Synthatase and GAT domain are unliganded in both structures. The water molecules W518 (X-ray) and W1 (MD) are present inside the oxyanion hole within a distance of ~0.77 Å.

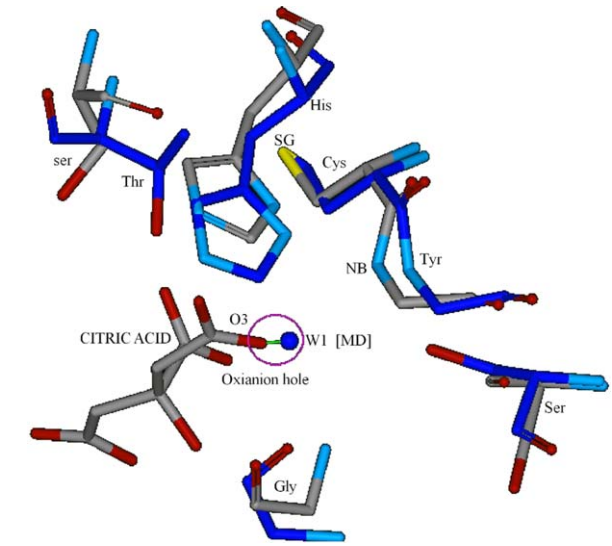

Figure 4
Superimposed (backbone atoms) structures of *Ec GMPS* (PDB Id. 1GPM) from X-ray and hGMPS (PDB Id. 2VPI) from MD simulation are shown in CPK and blue colours. The water molecule W1 (MD) of 2VPI structure is occupied inside the oxyanion hole of O3 atom of citric acid in crystal structure 1GPM (PDB Id.) within the distance ~0.66 Å in GAT domain. [Color figure can be viewed in the online issue, which is available at wileyonlinelibrary.com.]

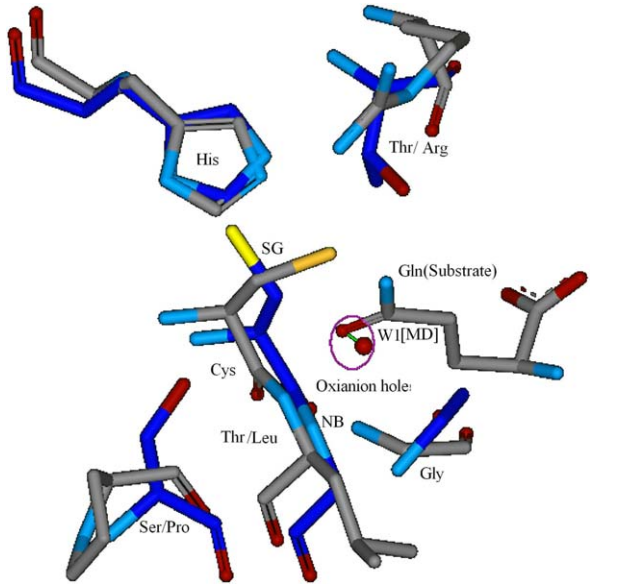

Figure 5

Superimposed (backbone atoms) structures of *TtCPS* (PDB Id.1VCO) from X-ray and hGMPS (PDB Id. 2VPI) from MD simulation are shown in CPK and blue colours. The water molecule W1 (MD) of 2VPI structure is occupied inside the oxyanion hole of O3 atom of citric acid in crystal structure 1VCO (PDB Id.) within the distance ~0.47 Å in GAT domain. The PDB Id. 1VCO is the only available crystal structure that represents the Conformation 1. [Color figure can be viewed in the online issue, which is available at wileyonlinelibrary.com.]

bonding interaction. The water molecules that interact with Ser75, His195, and Thr152 are considered as WS, WH and WTA/WTB, whereas the water molecule that bridges WH and W1 is designated as W2A (Supporting Information Fig. S4). In 1A conformation, it was observed that W1, which occupies the oxyanion pocket, is stabilized by water molecules WS and W2A, that further interact with Ser75 and WH. The His190 (NE) interacts with Thr152 (OG) via WH and W2A, but both residues stabilize the W1 water center through the network of interactions WH—W2A—W1 and WTA—WH—W2A—W1. Subsequently, conformation of 1B indicates that the oxyanion pocket, especially W1 water molecule, is stabilized by interactions with Ser75 (OG), W2B and WTB. The current scenario indicates that His190 and Thr152 are not involved in interaction with each other, else these residues would associate to stabilize W1 through interactions His190—WH—W2B—W1 and Thr152—WTB—W1. The details of inter-atomic interactions observed in conformations 1A and 1B are shown in Figure 6. To highlight the structural movement of each residue inside the oxyanion pocket, each conformation (1A/1B) has been superimposed on the initial (X-ray) structure. The complex between X-ray structure with conformation 1A (RMSD 1.9 Å) and 1B (RMSD 1.0 Å) indicates reasonable movement of Thr152 during the simulation, however, dynamics of other residues of oxyanion pocket are not significant. The MD results reveal that Thr152 moves away from the concerned pocket in

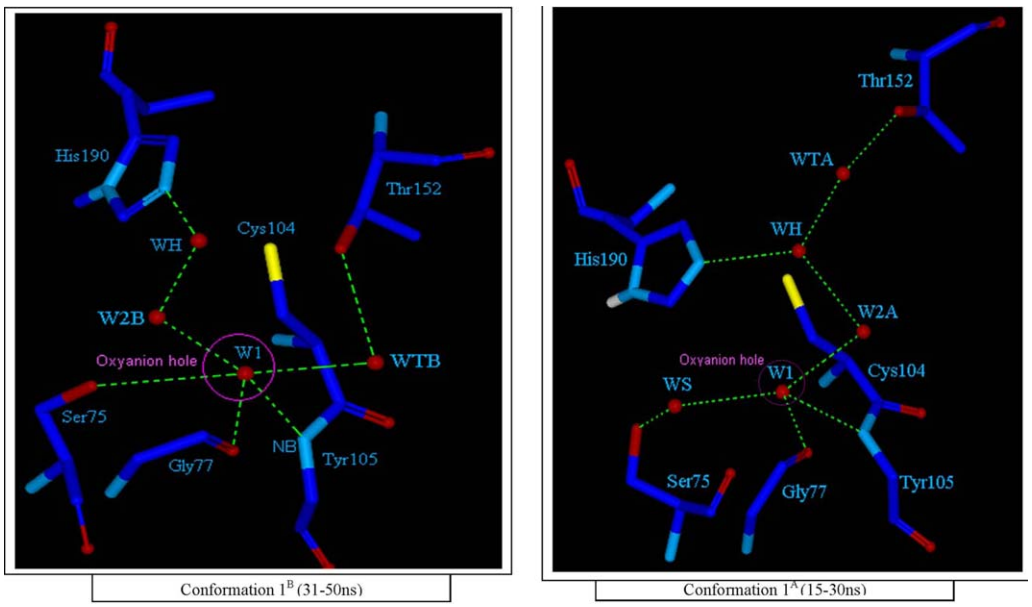

Figure 6

The left and right panels indicate the conformation of 1^B and 1^A in MD structures of 2VPI (PDB Id.). The W1 of oxyanion pocket interactions with Thr152 (by three conserved water molecules W2A,WH and WTA), Gly77, His190 (through W2A and WH) and Ser75 (by WS) in Conformation 1A. W1 interacts with Thr152 (by one conserved water molecule WTB), His190 (by W2B and WH), Gly77 and Ser75 in Conformation 1B.

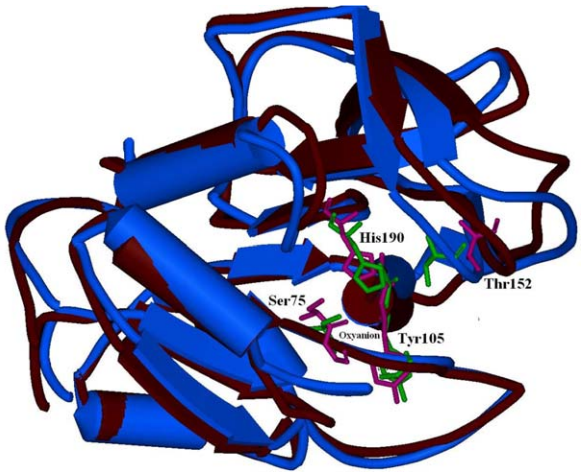

Figure 7

Superimposed MD structures of conformation 1A (brown) and 1B (blue) from the entire GAT domain. The significant movement of Thr152 from conformation 1A (pink) to 1B (green) is observed during MD simulation. [Color figure can be viewed in the online issue, which is available at wileyonlinelibrary.com.]

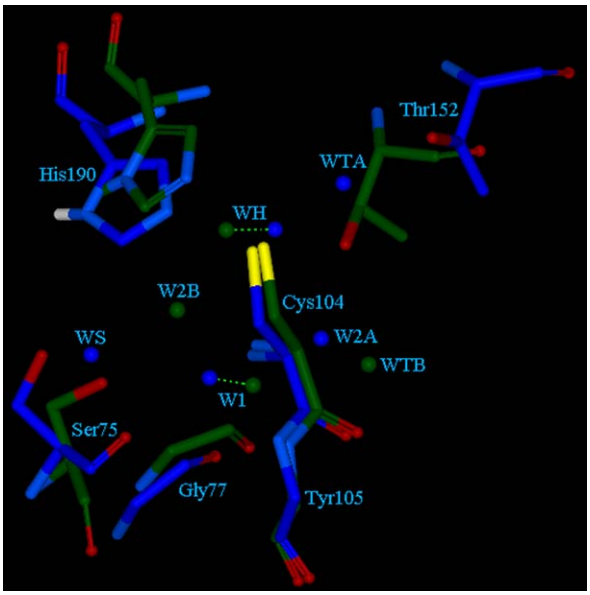

Figure 8

The conserved position of water molecules in the superimposed MD structures of Conformation 1A (blue) and 1B (green). The position of W1 and WH are conserved in both conformation because distance from W green to blue is 1.5 Å.

conformation 1A, but it again comes closer to the oxyanion pocket for stabilization of the primary catalytic region in 1B conformation (Fig. 7). During the simulation, the conformation 1A is observed between 15 ns to 35 ns, which then undergoes transition to conformation 1B and is observed from 35 to 50 ns.

Dynamics of water molecules

The superimposed structures of conformation 1A and 1B indicate that the position of water molecules seems to be conserved either in conformation 1A/1B or 1A and 1B (Fig. 8). Interestingly, W1 and WH water molecules are conserved during the entire simulation with a lifetime of 15–50 ns and their average SASA values are 7.4 and 19.01Å^2. But W2A and WTA are found only in conformation 1A, whereas W2B and WTB are present in conformation 1B. The average SASA values of corresponding W2A, W2B, WS, and WTB water molecules are 28.97, 16.42, 17.05 and 44.33 15.76 Å^2, respectively (Table III). The SASA value of W1 indicates that the position of this site is tightly enveloped by other residues and it seems to be a structural buried water molecule while others may act as surface water molecules. Interestingly, the role of water molecules W2A (conformation 1A) and W2B (conformation 1B) are significant as they also participate in linking WH and W1 water centers to bridge the oxyanion pocket with His190. In addition, WS and WTA which are observed in conformation 1A, may be responsible for stabilization of Ser75 at the oxyanion pocket.

Analysis of conformational energy, structural flexibility and dihedral angle

The NAMD energy tool in VMD program was used to calculate the conformational energy of 1A and 1B MD structures (15 to 50 ns) without the bulk solvent and the difference in conformational energy of 1A and 1B is shown in Supporting Information Figure S5. It indicates that the entire system is stable and the variation in conformational energy from initial to final state ($\Delta\Delta$Ec) is $\pm$ 20 kcal/mol. The N and C terminal region of GAT domain show most flexibility during the simulation; however in conformation 1A, the atomic fluctuations (CA atom only) of Thr152 and Gly215 are 2 and 2.5 Å. In conformation 1B, the fluctuation of Ala35, Gly77,

Table III

Conserved Hydrophilic Position of the Water Molecules, Their Lifetime and Average SASA (Solvent Accessible Surface Area was calculated) Values (Å^2) in MD Structure of 2VPI (PDB Id.)

Structurally equivalent water molecules		Life time of water molecules (ns)	SASA(Å^2)
Conformation 1A	Conformation 1B		
W1	W1	15–50	7.44
WH	WH	15–50	19.01
W2A	Nil	15–30	28.97
Nil	W2B	31–50	16.42
Nil	WS	31–50	17.05
WTA	Nil	15–30	44.33
Nil	WTB	31–50	15.76

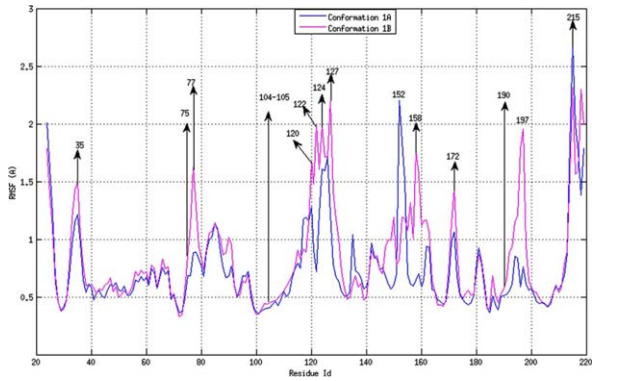

Figure 9

Comparison of Cα RMSF (root-mean-square fluctuation) value (Å) of each residue for the conformation 1A (blue) and 1B (pink) obtained from MD simulation (15 to 50 ns). [* The important residues, Res id: Ala35, Ser75,Gly76,Gly77,Cys104,Tyr105,Gly106, Lys120, Ser122, Arg124,Gly127, Thr152, Asp158, His153, Asn172, His190, Glu197, and Gly215 have been marked in the figure]. [Color figure can be viewed in the online issue, which is available at wileyonlinelibrary.com.]

Lys120, Ser122, Arg124, Gly127, Asp158, Asn172, and Leu195 are observed to vary from 1.5 to 2.2 Å. The flexibility of each residue and their RMSF values are plotted in Figure 9. The calculated RMSF from X-ray structure is reasonably defined with an average fluctuation of ∼1 Å, but the region between residues 77 to 85, which has no electron density for the corresponding CA atoms, is represented as showing zero fluctuation (Supporting Information Fig. S6). The present investigation is centered on oxyanion pocket and its surrounding residues, since flexibility or atomic fluctuation of GAT domain is significant only in this region. The oxyanion pocket predominantly consists of NB atom of Tyr105, hence we calculated the distances from $Tyr105^{NB}$ to $His190^{NE}$, $Gly77^{OB}$, $Ser75^{OG}$ and $Thr152^{OG}$, which are shown in Supporting Information Figure S7. The distances from $Tyr105^{NB}$ to $His190^{NE}$/$Gly77^{OB}$/$Ser75^{OG}$/$Thr152^{OG}$ are 6.59/4.99/5.93/9.4 Å, respectively, for conformation 1A, whereas these distances are 6.78/4.92/5.82/6.2 Å, respectively, in conformation 1B (Table IV). Furthermore, the MD results have confirmed that significant movement of Thr152 is observed during the transition from conformation 1A to 1B, as suggested by large RMSF of Thr152 and its distance with respect to Tyr105. The variation of chi1 dihedral angles is shown in Supporting Information Figures S8 and S9. Interestingly, the dihedral angle/chi1 values that are observed during simulation vary between −10° to 30°for Ser75, −90° to −50° for His190, and 20° to 35° for Cys104, but the chi1 value for Cys104 decreased to −10° during 24 to 27 ns simulation. Again, the rotation of chi1 value of Thr152 is interesting because the chi1 value in conformation 1A varies from −20° to 40° and suddenly increases to vary between 80 and 100° in conformation 1B. So, the change in dihedral angle chi1 of Thr152 is mostly favorable, and also agrees with the large RMSF value and variation in distance from NB atom of Tyr105.

Analysis of mutant structures

The non catalytic residue Ser75 may induce hydrophilicity at oxyanion hole and possibly supplies the W1 water molecule in conformation 1B to maintain the topology of this pocket. To investigate the functional role of Ser75 and examine the role of W1 water molecule inside the pocket, mutation of Ser75 to Val was carried out. The results of MD simulations of mutant (Ser75Val) structure indicate that the W1 water molecule is not found inside the oxyanion pocket because the bulky hydrophobic side-chain of Val75 and resultant stereochemical constraints may create a potential barrier to the entry of a water molecule into the oxyanion pocket. The WTB and WH waters are observed to interact with Thr152 and His190 during the entire simulation (upto 25 ns), but these water molecules are not observed to interlink with oxyanion hole; moreover, W2B is also inaccessible in conformation 1B. However, no other significant conformational change is found during the simulation, rather the oxyanion pocket seems destabilized due to the absence of water molecules at the pocket. So, the side-chain of Ser75 seems to act as a gate keeper of the oxyanion pocket and also maintains the hydrophilic environment surrounding this pocket. The fluctuation of CA atoms of MD mutant structure is presented in Figure

Table IV

Interactions Between Tyr105 (NB) to Thr152 (OG), Gly77 (OB), Ser75 (OG), and the Water Mediated Bridges Involving Them

Conformation/residential time		Interaction of Tyr105 with other residues			
		$_{NB}Tyr^{105}$– $_{NE}His^{190}$	$_{NB}Tyr^{105}$—$_{OG}Thr^{152}$	$_{NB}Tyr^{105}$—$_{OB}Gly^{77}$	$_{NB}Tyr^{105}$—$_{OG}Ser^{75}$
1^{A} (15-30ns)	Distance (Å)	6.59	9.4	4.99	5.93
	Water bridges	3	4	1	2
		(W1,W2A,WH)	(W1,W2A, WH, WTA)	(W1)	(W1,WS)
1^{B} (31-50ns)	Distance (Å)	6.78	6.2	4.92	5.82
	Water bridges	3	2	1	1
		(W1,W2B,WH)	(W1,WTB)	(W1)	(W1)

The average distances (Å) are measured in conformation 1A and 1B.

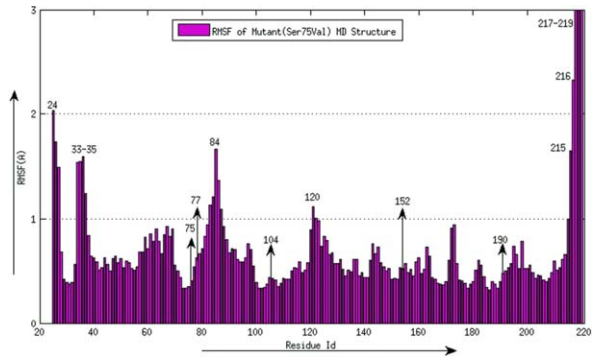

Figure 10

The Cα RMSF values (Å) of mutant (Val75Ser) MD structure. The important residues are marked in the figure. [*The Res id: Met24, Ala33, Gly34, Ala35, Ser75, Gly77, Glu84, Cys104, Lys120, Thr152, His190, Gly215, Thr216, Phe217, Thr218, Val219 marked in the figure]. [Color figure can be viewed in the online issue, which is available at wileyonlinelibrary.com.]

10. Reasonable movement (within 1 Å) is observed for most residues, except Met24, Ala33, Gly34, Glu84, Lys120, Gly215, Thr216 whose RMSF values vary between 1 to 2 Å, and Phe217, Thr218, and Val219, whose fluctuations are ~3 Å.

DISCUSSION

The focus of the present study is on the oxyanion pocket of GAT domain in hGMPS enzyme, so as to characterize its stabilization, participation in reaction mechanism, change of conformation and the role of water molecules during the molecular dynamics simulation. Comprehensive analysis of various crystal structures of GMPS enzyme clearly demonstrates the change of conformation, especially movement of the side-chain of catalytic Cys (res.Id 104/86/78/391) residues to switch from its non-functional to functional form.[49] The ligands at synthatase domain may influence the catalytic machinery system (especially its Cys/His residues) of GAT domain to adopt conformations in readiness for chemical reaction. Biochemical and structural studies suggest that after invading into the GAT domain, the substrate (Gln) initiates the enzymatic reaction mechanism and forms a tetrahedral intermediate where negatively charged oxyanion (O^-) of the substrate is stabilized by interaction with the positively charged backbone (NB) atoms of the residues Tyr105 and Gly77.[13] The MD results and various analyses (such as RMSD values, superimposed structures between crystal and MD average, change of conformation energy, calculation of the distances from oxyanion hole to other residues, dihedral angle of respective residues and finally calculation of flexibility/RMSF of residues forming the oxyanion pockets) have confirmed the existence of two conformations of oxyanion pocket in the GAT domain of hGMPS enzyme. During dynamics, the oxyanion pocket adopts two conformations (1A and 1B) to stabilize the catalytic system in the absence of ligands. The average volumes of the concerned pockets, especially the free spaces of average volumes are observed to be 82Å^3 for Conformation 1A and 140Å^3 for 1B (Fig. 11). Generally, the volumes of oxyanion pockets are ~70 to 90Å^3, as observed in different crystal structures of oxyanion-binding proteins.[50] As a crude approximation, we estimated the size of pocket, required to bind water molecule by calculating the volume of a "minimal sphere."

Moreover, the change of conformation of GAT domain (in hGMPS enzyme) from its ligand bound (crystal structure) to unliganded state (MD structures) is unidirectional, with the final conformation being retained and stabilized by several conserved water molecules and interactions involving Ser75 and Thr152. The position of oxyanion (that is formed in the tetrahedral intermediate state and for which no crystal structure is available to represent this state) is occupied by water molecule W1 when the substrate is absent. Moreover other water

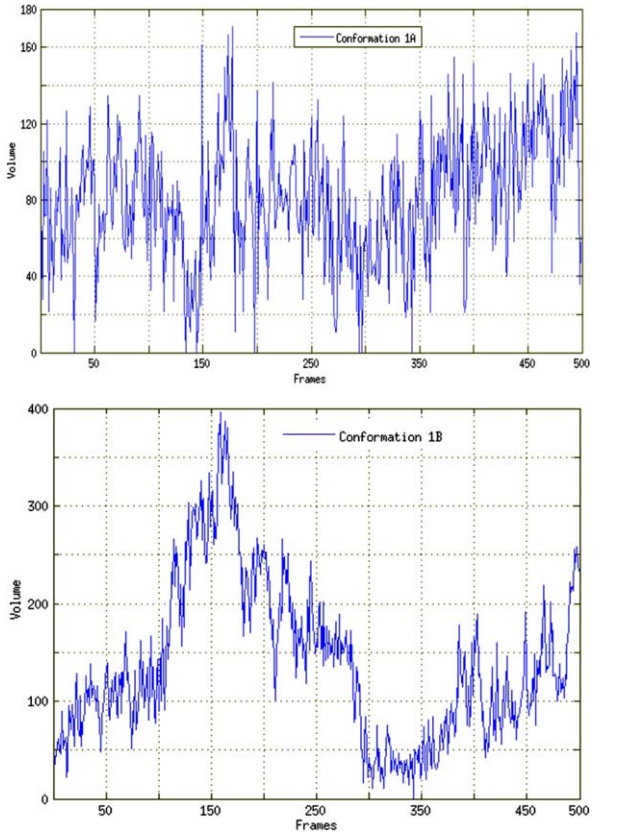

Figure 11

Comparison of volumes (Å^3) for oxyanion pocket in MD-simulated structures. Top and lower panels shown the conformation 1A and 1B. The final 500 frames were obtained from each conformation for calculation of volume. [Color figure can be viewed in the online issue, which is available at wileyonlinelibrary.com.]

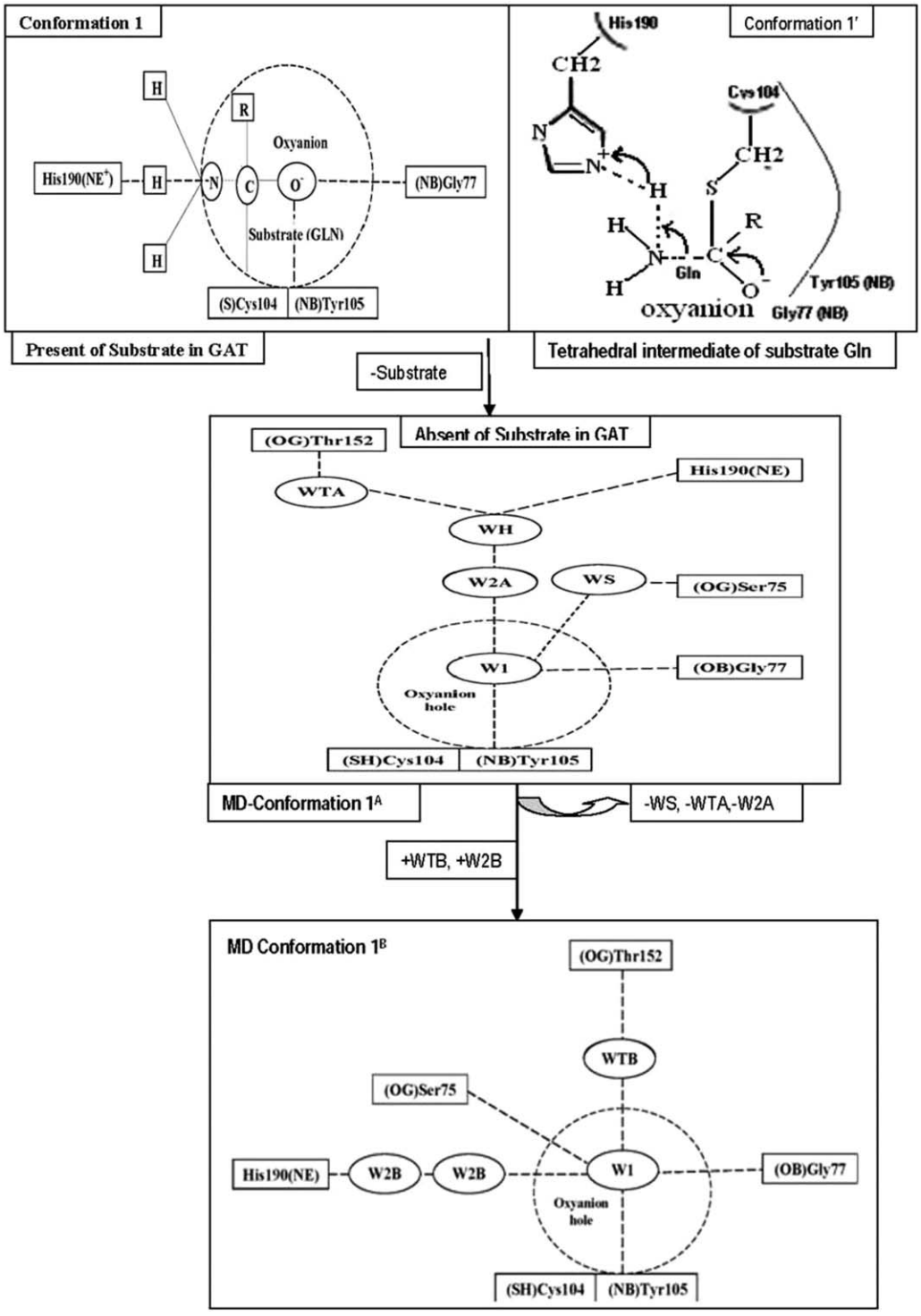

Figure 12

Schematic representation of oxyanion hole and interactions with different residues. The top left and right panels shown conformation 1 and 1'. The oxyanion of Gln (substrate) is stabilized by NB atoms of Tyr105 and Gly77 residues at the presence of Gln in GAT domain. The middle and lower panels indicate the Conformation 1A and 1B (corresponding figure 6) and shown the interactions with conserved water molecule W1 (which occupied at the position of oxyanion of Gln) with its surrounding residues in MD structure of GAT domain.

molecules WS, W2A, WH, WTA also get associated to maintain the architecture of conformation 1A. In addition, during the time of transition from conformation 1A to 1B, WS, WTA, W2A water molecules are expelled from their positions, and subsequently water molecules WTB and W2B enter the pocket to sustain the geometrical features of conformation 1B. But the position of W1 water molecule, that remains unchanged from that observed in conformation 1A, is stabilized by presence of water molecules WTB, W2B, WH in conformation 1B (Fig. 12). Furthermore, the W1 hydrophilic position has a propensity to be occupied by a water molecule in the presence of Ser75 at GAT domain; in contrast, mutation of Ser75 to Val may be thought to reduce the hydrophilicity of the oxyanion pocket, thus creating a potential barrier against the entry of water molecules into the pocket. Possibly, the hydrophilicity of the oxyanion pocket may be generated by the movement of Ser75 and Thr152 that may induce the water molecules to change their geometrical positions. However, the surrounding residues of oxyanion pocket were apparently thought to be nonessential for catalytic activity (in stabilizing the negatively charged group of the substrate) of GAT domain, but our MD studies confirmed that Ser75 and Thr152 may be responsible for tuning the change of conformation during simulation, and they may act as catalytic partners along with Cys104 and His190 of human GMPS enzyme. So, the mutual coupling of catalytic residues with non catalytic partners and their conserved water mediated intricate involvement could possibly provide some pointers for future biochemical or experimental assays to validate or compare our arguments toward better understanding the molecular basis of the enzyme action. The stereochemical features and topologies of the conserved water molecules and their positions inside the oxyanion pocket of GAT domain may also facilitate future drug discovery by design of appropriately oriented chemical groups with suitable spacer length that may mimic the structural and electronic properties of these conserved water centers.

CONCLUSIONS

MD-results suggest that the position of oxyanion (unliganded conformation of hGMPS enzyme) is occupied by one conserved water molecule (W1), which also stabilizes the oxyanion pocket, while this position (water center) is occupied by a negatively charged atom of the substrate or ligand in ligand bound state. Interestingly, the conserved water molecule may be supplied by Ser75, whereas Thr152 and His190 can also act as anchor residues to maintain stereo chemical architecture of oxyanion pocket through conserved water mediated H-bonding interaction. Subsequently, hydroxyl groups of Ser75, Thr152 and imidazole group of His190 may control the structural integrity and electronic consequences of the primary catalytic zone of GAT domain. Possibly, four conserved water molecules may stabilize the oxyanion hole in unliganded state, but they move and vacate the positions when enzyme (hGMPS)-substrate complex is formed. So, MD results have confirmed the significant role of conserved water molecules at the catalytic region of GAT domain and their active participation in recognition of oxyanion pocket, along with the non-catalytic residues (Ser75 and Thr152), which may provide new biochemical insights about the hGMPS enzyme. Our computational investigations have clearly revealed that, the negatively charged atom of substrate or oxyanion (O^-) is stabilized by positively charged backbone atoms (NB) of oxyanion hole in enzyme-(GMPS)-substrate complex, while in the absence of a substrate, the oxyanion position will definitely be occupied by oxygen atom of a single conserved water molecule that is thought to be supplied by the surrounding hydrophilic residues of the enzyme. The results from this computational study could be of interest to experimental community and also provide a testable hypothesis for experimental validation. The conserved hydrophilic sites (water molecules) near oxyanion hole highlight the structural importance of water molecules, suggesting a possible need for changing the conventional definition of chemical geometry of inhibitor binding site, its shape and complimentarity.

ACKNOWLEDGMENT

HRB is thankful to Science and Engineering Research Board (Department of Science and Technology, Govt. of India) for providing financial support to the Research Project SB/FT/CS-051/2012. Authors thank the Supercomputer Education and Research Centre, Indian Institute of Science and DBT-IISc Partnership Programme, for providing the computing resources.

REFERENCES

1. Hirst M, Haliday E, Nakamura J, Lou L. Human GMP synthetase protein purification, cloning, and functional expression of cDNA. J Biol Chem 1994;269:2383–23837.
2. Hedstrom L. IMP dehydrogenase: structure, mechanism and inhibition. Chem Rev 2009;109:2903–2928.
3. Reddy BA, Knaap JAV, Bot AGM. Nucleotide biosynthetic enzyme GMP synthase is a TRIM21-controlled relay of p53 stabilization. Mol Cell 2014;53:458–470.
4. Weber G, Nakamura H, Natsumeda Y, Szekeres T, Nagai M. Regulation of GTP biosynthesis. Adv Enzyme Regul 1992;32:57–69.
5. Lou L, Nakamura J, Tsing S, Nguyen B, Chow J, Straub K, Chan H, Barnett J. High-level production from a baculovirus expression system and biochemical characterization of human GMP synthetase. Protein Expr Purif 1995;6:487–495.
6. Weber G, Prajda N. Targeted and non-targeted actions of anticancer drugs. Adv Enzyme Regul 1994;34:71–89.
7. Welin M, Lehtiö L, Johansson A, Flodin S, Nyman T, Trésaugues L, Hammarström M, Gräslund S, Nordlund P. Substrate specificity and oligomerization of human GMP synthetase. J Mol Biol 2013;15: 4323–4333.

8. Griffiths M, Keast D. The effects of a leukaemia-controlling dose of acivicin on murine splenic lymphocytes in vitro and in vivo. Immunol Cell Biol 1991;69:395–402.
9. Chittur SV, Klem TJ, Shafer CM, Davisson VJ. Mechanism for acivicin inactivation of triad glutamine amidotransferases. Biochemistry 2001;40:876–887.
10. Huang X, Holden HM, Raushel FM. Channeling of substrates and intermediates in enzyme-catalyzed reactions. Annu Rev Biochem 2001;70:149–180.
11. Nakamura J, Lou L. Biochemical characterization of human GMP synthetase. J Biol Chem 1995;270:7347–7353.
12. Nakamura J, Straub K, Wu J, Lou L. The Glutamine Hydrolysis Function of Human GMP Synthetase Identification of an essential active site cysteine. J Biol Chem 1995;270:23450–23455.
13. Tesmer JJ, Klem TJ, Deras ML, Davisson VJ, Smith JL. The crystal structure of GMP synthetase reveals a novel catalytic triad and is a structural paradigm for two enzyme families. Nat Struct Biol 1996;3:74–86.
14. Mouilleron S, Golinelli-Pimpaneau B. Conformational changes in ammonia-channeling glutamine amidotransferases. Curr Opin Struct Biol 2007;17:653–664.
15. Oliver JC, Gudihal R, Burgner JW, Pedley AM, Zwierko AT, Davisson VJ, Linger RS. Conformational changes involving ammonia tunnel formation and allosteric control in GMP synthetase. Arch Biochem Biophys 2014;1:22–32.
16. Oliver JC, Linger RS, Chittur SV, Davisson VJ. Substrate activation and conformational dynamics of guanosine 5'-monophosphate synthetase. Biochemistry 2013;6:5225–5235.
17. Bhat JY, Venkatachala R, Singh K, Gupta K, Sarma SP, Balaram H. Ammonia channeling in Plasmodium falciparum GMP synthetase: investigation by NMR spectroscopy and biochemical assays. Biochemistry 2011;26:3346–3356.
18. Ali R, Kumar S, Balaram H, Sarma SP. Solution nuclear magnetic resonance structure of the GATase subunit and structural basis of the interaction between GATase and ATPPase subunits in a two-subunit-type GMPS from Methanocaldococcus jannaschii. Biochemistry 2013;25:4308–4323.
19. Hart E, Powers-Lee SG. (Mutation analysis of carbamoyl phosphate synthetase: Does the structurally conserved glutamine amidotransferase triad act as a functional dyad? Protein Sci 2008;17:1120–1128.
20. Goto M, Omi R, Nakagawa N, Miyahara I, Hirotsu K. Crystal structures of CTP synthetase reveal ATP, UTP, and glutamine binding sites. Structure 2004;12:1413–1423.
21. Bairagya HR, Mukhopadhyay BP. An insight to the dynamics of conserved water mediated salt bridge interaction and interdomain recognition in hIMPDH isoforms. J Biomol Struct Dyn 2013;31:788–808.
22. Bairagya HR, Mishra DK, Mukhopadhyay BP, Sekar K. Conserved water-mediated recognition and dynamics of NAD^+ (carboxamide group) to hIMPDH enzyme: water mimic approach toward the design of isoform-selective inhibitor. J Biomol Struct Dyn 2014;32:1248–1262.
23. Bairagya HR, Mukhopadhyay BP. Protein folding: challenge to chemistry. J Biomol Struct Dyn 2013;31:993–994.
24. Farrell PO, Joshua-Tor L. Mutagenesis and crystallographic studies of the catalytic residues of the papain family protease bleomycin hydrolase: new insights into active – site structure. Biochem J 2007; 401:421–428.
25. Berman HM, Westbrook J, Feng Z, Gilliand G, Bhat TN, Weissig H, Shindyalov IN, Bourne PE. The Protein Data Bank. Nat Struct Biol 2003;10:980
26. Berman HM, Westbrook J, Feng Z, Gilliand G, Bhat TN, Weissig H, Shindyalov IN, Bourne PE. The Protein Data Bank. Nucleic Acids Res 2000;28:235–242.
27. Bernstein FC, Koetzle TF, Williams, Jr, GJ, Meyer EF, Brice MD, Rodgers JR, Kennard O, Shimanouchi T, Tasumi M. The Protein Data Bank: a computer-based archival file for macromolecular structures. J Mol Biol 1997;112:535–542.
28. Guex N, Diemand A, Peitsch MC, Schwede T. SwissPDBViewer program. Glaxo Smith Kline R. &D, 2000.
29. Guex N, Peitsch MC. SWISS-MODEL and the Swiss-PdbViewer: an environment for comparative protein modeling. Electrophoresis 1997;18:2714–2723.
30. Kleywegt GJ, Jones TA. Model-building and refinement practice. Methods Enzymol 1997;277:208–230.
31. Humphrey W, Dalke A, Schulten K. VMD: visual molecular dynamics. J Mol Graph 1996;14:33–38.
32. Kale L, Skeel R, Bhandarkar M, Brunner R, Gursoy A, Krawetz N, Phillips J, Shinozaki A, Krishnan V, Schulten K. NAMD2: greater scalability for parallel molecular dynamics. J Comput Phys 1999;151:283–312.
33. Leroux V, Gresh N, Liu WQ, Garbay C, Maigret B. Role of water molecules for binding inhibitors in the SH2 domain of Grb2: a molecular dynamics study. J. Theo Chem 2007;806:51–66.
34. Brooks BR, Bruccoleri RE, Olafson BD, States DJ, Swaminathan S, Karplus M. (Charmm - a program for macromolecular energy, minimization, and dynamics calculations. J Comput Chem 1983;4:187–217.
35. MacKerell Jr, AD, Bashford D, Bellott M, Dunbrack JRL, Evanseck JD, Field MJ, Fischer S, Gao J, Guo H, Ha S, Joseph-McCarthy D, Kuchnir L, Kuczera K, Lau FTK, Mattos C, Michnick S, Ngo T, Nguyen DT, Prodhom B, Reiher WE, Roux B, Schlenkrich M, Smith JC, Stote R, Straub J, Watanabe M, Wiórkiewicz-Kuczera J, Yin D, Karplus M. All-Atom Empirical Potential for Molecular Modeling and Dynamics Studies of Proteins. J Phys Chem B 1998;102: 3586–3616.
36. Grest GS, Kremer K. Molecular-dynamics simulation for polymers in the presence of heat bath. Phys Rev 1986;33:3628–3631.
37. Feller SE, Zhang YH, Pastor RW, Brooks BR. (Constant pressure molecular dynamics simulation—the langevin piston method. J Chem Phys 1995;103:4613–4621.
38. Martyna GJ, Tobias DJ, Klein ML. Constant pressure molecular dynamics algorithms. J Chem Phys 1994;101:4177–4189.
39. Allen MP, Tildesley DJ. Computer simulation of liquids, Oxford: Clarendon Press; 1987.
40. Dongsheng L, Xing Z, Shengbo J. Structural features of cholesteryl ester transfer protein: A molecular dynamics simulation study. Proteins 2013;81:415–425.
41. Sumathi K, Ananthalakshmi P, Roshan MMNA, Sekar K. 3dSS: 3D structural superposition. Nucl Acids Res 2006;34:128–138.
42. Ogata K, Wodak SJ. Conserved water molecules in MHC class-I molecules and their putative structural and functional roles. Protein Eng 2002;15:697–705.
43. Doss CGP, Rajith B, Garwasis N, Mathew RP, Rajua AS, Apoorvaa K, Williama D, Sadhanaa NR, Himania T, Dikeb IP. Screening of mutations affecting protein stability and dynamics of FGFR1—A simulation analysis. Appl Transl Genomics 2012;1:37–43.
44. Wiederstein M, Sippl MJ. ProSA-web: interactive web service for the recognition of errors in three-dimensional structures of proteins. Nucleic Acids Res 2007;35:407–410.
45. Luthy R, Bowie JU, Eisenberg D. Assessment of protein models with three dimensional profiles. Nature 1992;356:83–85.
46. Benkert P, Kuenzli M, Schwede T. QMEAN server for protein model quality estimation. Nucleic Acids Res 2009;1:510–514.
47. Laskowski RA, MacArthur MW, Moss DS, Thornton JM. PROCHECK—a program to check the stereochemical quality of protein structures. J App Cryst 1993;26:283–291.
48. Laurent B, Chavent M, Cragnolini T, Dahl AC, Pasquali S, Derreumaux P, Sansom MS, Baaden M. (Epock: rapid analysis of protein pocket dynamics. Bioinformatics 2014;1–3. doi: 10.1093/bioinformatics/btu822.
49. Isupov MN, Obmolova G, Butterworth S, Badet-Denisot MA, Badet B, Polikarpov I, Littlechild JA, Teplyakov A. Substrate binding is required for assembly of the active conformation of the catalytic site in Ntn amidotransferases: evidence from the 1.8 A crystal structure of the glutaminase domain of glucosamine 6-phosphate synthase. Structure 1996;15:801–810.
50. Lawson DM, Williams CE, Mitchenall LA, Pau RN. Ligand size is a major determinant of specificity in periplasmic oxyanion-binding proteins: the 1.2Å resolution crystal structure of Azotobacter vinelandii ModA. Structure 1998;6:1529–1539.